Sci. Rep. Kanazawa Univ.
Vol. 41 No. 1 pp, 25~45
July 1996

Classification of peridotite xenoliths in calc-alkaline andesite from Iraya volcano, Batan Island, the Philippines, and its genetical implications

Shoji ARAI[1], Megumi KIDA[1], Natsue ABE[1], Atusi NINOMIYA[1] and G. P. Yumul, Jr.[2]

1 *Department of Earth Sciences, Faculty of Science, Kanazawa University, Kakuma, Kanazawa 920-11, Japan.*

2 *National Institute of Geological Sciences, University of the Philippines, College of Science, Diliman, Quezon City 1101, the Philippines.*

Abstract: The peridotite xenolithic suite in calc-alkaline andesite from Iraya volcano, the Philippines, is one of rare samples derived from wedge mantle. The Iraya peridotite xenoliths are classified into two types, F (fine-grained)-type and C (coarse-grained)-type, based on petrographic characteristics. The former peridotites (94%) overwhelm the latter (6%) in volume. The former peridotites have very peculiar textures; olivine is fine-grained and has numerous minute inclusions, and orthopyroxene, free of exsolution lamellae and deformation, is radially aggregated. This texture is very similar to that in peridotite hornfels (= deserpentinized peridotite). The C-type peridotites are mainly harzburgite with equigranular to porphyroclastic textures, equal to ordinary peridotite xenoliths documented from various localities. C-type peridotites have relatively uniform mineral chemistry; olivine varies from Fo_{91} to Fo_{92} and Cr/(Cr + Al) atomic ratio (= Cr#) of chromian spinel is from 0.5 to 0. 6. F-type peridotites, in contrast, have a wide compositional range; Fo of olivine varies from 89 to 93 and Cr# of spinel, from 0.4 to 0. 7. Orthopyroxene has lower contents of Ca, Al and Cr in F-type peridotites than in C-type ones. These textural and chemical characteristics indicate two possibilities for the origin of the F-type peridotites. One is a deserpentinization origin; abyssal serpentinite had been dehydrated due to heating after initiation of arc setting. C-type peridotites may be their protolith. Alternative is a metasomatism origin. Si-rich melt or fluid derived from slab had invaded the wedge mantle; the orthopyroxene low in Ca, Al and Cr particular to F-type peridotites was a reaction product between primary olivine and the melt/fluid.

1. Introduction

Mantle-derived xenoliths in volcanics give us direct information on deep processes

beneath the volcanoes. The mantle-xenolith carriers are, however, strongly biased to continental and oceanic hotspot areas (e. g., Nixon, 1987). There are only a few localities where xenoliths of mantle peridotites are available from arc magmas (Abe et al., 1993); Megata volcano (e. g., Hayashi, 1955 ; Kuno and Aoki, 1970 ; Takahashi, 1986) and Oshima-Oshima volcano (Ninomiya and Arai, 1992), Northeast Japan arc, Avacha volcano, Kamchatka (e. g., Shcheka, 1976), and Iraya volcano, the Philippines (e. g., Richard, 1986 ; Vidal et al., 1989). We can get plenty of xenoliths at Megata volcano (Ichinomegata, Ninomegata and Sannomegata craters), where detailed petrographical and petrological data have been available (e. g., Aoki and Prinz, 1974 ; Takahashi, 1978, 1980, 1986 ; Abe et al., 1992, 1995 ; Abe and Arai, 1993). The upper mantle peridotites beneath the Japan arcs are roughly similar in major-element mineral chemistry and degree of refractoriness to abyssal peridotites (e. g., Arai, 1991, 1994). Mantle metasomatism and hydration related to arc magmatism proceed within wedge mantle of the Northeast Japan arc (e. g., Abe et al., 1995a, b). Abe et al. (1995b) especially demonstrated that the Japan arc mantle peridotites have peculiar geochemical characteristics just intermediate between abyssal peridotites and oceanic hotspot or continental rift zone ones. We need more samples derived from wedge mantle to establish its petrological and geochemical signature in more general. As described below most of the peridotite xenoliths from Iraya volcano have the textures that are very rare in other xenoliths ever documented elsewhere. In this preliminary article we will describe their petrographical characteristics, on which we will classify the peridotites.

2. Geological and tectonic background

Batan is the main island of the Batanes Province (Batan islands), comprising the northernmost tip of the Philippine territory (Fig. 1). Batan island is mainly composed of effusive rocks from three volcanoes. Mahatao volcano, the oldest one, started to erupt on the Philippine Sea plate at Late Miocene, followed by the eruption of Matarem volcano at Pliocene to Early Pleistocene. Iraya volcano has been active from Late Pleistocene (Plate I-a) (Richards et al., 1986). These volcanoes belong to the Luzon-Taiwan arc, which stands on the Luzon micro-block where the South China Sea basin has been subducted through the Manila trench (Stephan et al., 1986).

Volcanic rocks from Batan island are basalt and andesite. The andesite is calc-alkaline and is especially high-K at the latest stage (<2Ma) of Iraya volcano (Richards et al., 1986). Richards (1986) reported xenoliths of gabbroic cumulates and peridotites from volcanics younger than Phase III (<1.5 Ma) of Iraya volcano. They are especially abundant in pyroclastics of the latest eruption (1480 B. P.) (Richards, 1986). Xenoliths were mainly obtained from cliffs at Song-Song Bay (Plate I-b, c), east of Mt. Iraya (Fig. 1). They were easily collected either directly from the cliffs of pyroclastics or as blocks fallen from outcrops at the beach.

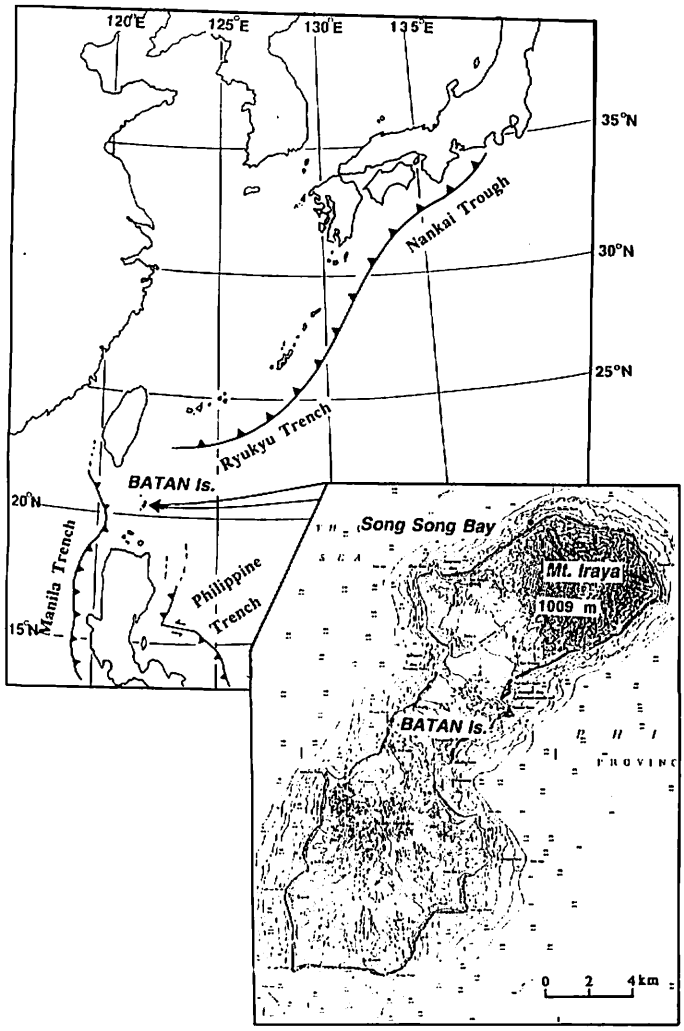

Fig. 1. Locality of Iraya volcano of Batan island, the Philippines.

3. Petrography

3. 1 Host rocks

The host rock for the peridotite xenoliths from Iraya volcano is calc-alkaline andesite (e.g., Richard, 1986). The andesite forms pyroclastic flow deposits at Song-Song Bay (Plate I-b, c). The essential ejecta have phenocrysts of plagioclase, augite, hypersthene, hornblende, olivine and magnetite (Plate I-e). Plagioclase frequently has a remarkable zonal structure with some dusty zones (Plate I-f). Olivine is usually euhedral and has minute inclusions of chromian spinel (Plate I-g). Hypersthene sometimes has thin reaction rim of clinopyroxene. Hornblende has brown color with weak greenish tint (Plate I-h).

Possible accessary andesitic blocks within the pyroclastic flow deposits also have peridotite and gabbro xenoliths (Plate I-d). They have phenocrysts of plagioclase, hornblende, augite, biotite and magnetite. Plagioclase shows remarkable oscillatory zoning and has dusty glass inclusions. Hornblende is yellowish to reddish brown under the microscope. Hornblende and biotite are partly or wholly opacitized (Plate I-f). Augite and magnetite sometimes make aggregates. Apatite is common as a microphenocryst. Groundmass is composed of plagioclase, clinopyroxene, magnetite and glass.

3. 2 Xenoliths

The largest is a peridotite xenolith of F-type (see below) and weighs 5.6 kg (Plate II-a). Xenoliths are classified into peridotites and gabbros. It is notable that they are frequently composite (Irving, 1980); peridotites are frequently veined and enclosed by gabbroic rocks (Plate II-b). Similar composite xenoliths were found in the Nishiyama andesite flow of Oshima-Oshima volcano, northern Japan (Plate II-b). Gabbroic xenoliths very frequently contain small angular clasts of peridotites, which are digested to various degrees (Plate II-b, c). The gabbro-peridotite relationship is, however, very complicated; gabbro with plenty of small peridotite clasts (or peridotite densely veined by gabbro or related hornblendite) is as a whole enclosed by another gabbro in some cases (Plate II-e).

Dark hornblendite is always formed at the contact between peridotite and gabbro (Plate II-c, e). Aggregates of hornblende frequently observed in gabbros are possibly equivalent to totally digested peridotite clasts (Plate II-d). The hornblendite selvage is also usually present between peridotite and andesite host. The color of the peridotite is pale yellow but is dark yellow when the hornblendite selvage is thick due to prevalent digestion by gabbroic magma (Plate II-c). The boundary of peridotite xenolith to the hornblendite selvage is sharp in the former and is obscure in the latter (Plate II-c).

Peridotite xenoliths can be classified into two types in terms of grain size of olivine; C (= coarse-grained)-type (Plate III-a) and F (= fine-grained)-type (Plate III-b). The C-type peridotites are composed of relatively coarse (up to several millimeters across) olivine and orthopyroxene and may be equivalent to "ordinary" mantle-derived peridotite xenoliths obtained from various localities (e. g., Nixon, 1987; Abe et al., 1993) (Plate III-a, c). The F-type peridotite xenoliths are basically composed of relatively fine-grained (less than 1 millimeter across) olivine (Plate III-d) with irregular-shaped gray speckles several millimeters across (Plate III-b). Color of olivine is paler in F-type (pale yellow) than in C-type (pale greenish yellow) (Plate III-e). Clinopyroxene is rather rare in the peridotite suite, especially in C-type peridotites, which are typical harzburgite (Plate III-a, c). Harzburgite is highly predominant over dunite. Both types of peridotites have small amount of chromian spinel. F-type peridotites are highly predominant over C-type ones: the volume ratio of the former to the latter is 0.94 to 0.06 based on the volume analysis for all (423) peridotite xenoliths arbitrarily sampled at Song-Song Bay. It is noteworthy that peridotites with intermediate characteristics (Plate V-c) which are very common were included in F-type peridotites in this article.

The C-type peridotites have coarse equigranular to porphyroclastic textures (Plate III-c). Coarse olivines in peridotites of C-type and of F-type (intermediate type) contain possible fluid inclusion trails, which are associated with minute orthopyroxene dots (Plate V-a, b). Orthopyroxene, which is frequently kinked, has prominent exsolution lamellae of clinopyroxene (Plate III-c, f). Small amount of clinopyroxene is present, frequently associated with orthopyroxene or chromian spinel (Plate III-g). Chromian spinel is anhedral (Plate III-h) or, less frequently, euhedral. Small amount of melt infiltrated along

grain boundaries and was reacted with chromian spinel and orthopyroxene to produce fine-grained minerals. The C-type peridotites are equal to ordinary equigranular to porphyroclastic peridotite xenoliths ever documented in both macroscopic and microscopic characteristics.

The F-type peridotites have extraordinary textural characteristics. Olivine is fine-grained (Plate III-b, d) and has numerous minute inclusions, which are rounded and concentrated in the central part of each grain (Plate V-d). These grains sometimes have the same optical orientation within an area of a few square millimeters to a square centimeter. Mode of occurrence of orthopyroxene is especially peculiar to this type of peridotite. Orthopyroxene, totally free of clinopyroxene lamellae but with inclusions of olivine and other minerals, frequently makes radial aggregates (Plate II-g, h : Plate IV-c ; Plate V-e, f). This texture has not been reported in peridotite xenoliths but is very common to peridotites made by deserpentinization (e. g., Arai, 1975 ; Matsumoto et al., 1995) (Plate V-g). Orthopyroxene also replaces olivine as veinlets or acicular crystals (Plate IV-d to -h). Orthopyroxene associated with hornblende rarely makes a network within F-type peridotite (Plate V-h ; Plate IV-a, b). The dark gray speckles (Plate III-b ; Plate VI-e, f) are usually composed of orthopyroxene, sometimes aggregated radially, with minute inclusions of chromian spinel (Plate V-a, b). Small anhedral to euhedral chromian spinel usually makes aggregates with interstitial hydrous mineral(s) ; its whole shape is very similar to that of chromian spinel in C-type

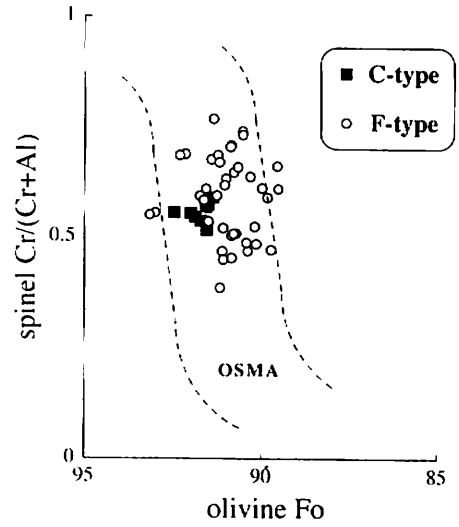

Fig. 2. Relationship between the Fo content of olivine and the Cr/(Cr + Al) atomic ratio of coexisting spinel. Note that C-type peridotites are confined within the olivine-spinel mantle array (OSMA), which is the mantle spinel peridotite restite trend (Arai, 1987, 1994).

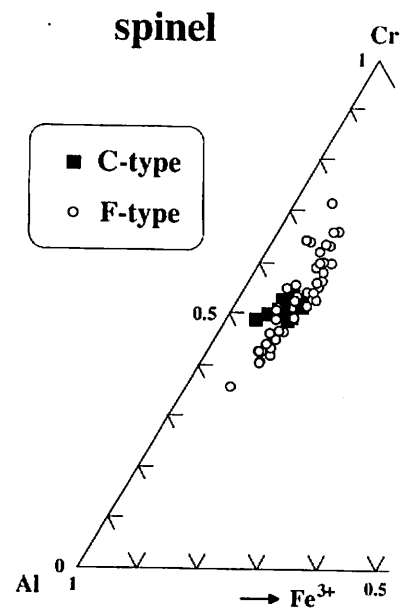

Fig. 3. Ratio of trivalent cations of chromian spinel in the peridotite xenoliths from Iraya volcano, the Philippines.

peridotite (Plate VI-c). Small amount of Ni-Fe sulfide (pentlandite) is commonly found in F-type peridotites. Hydrous minerals (pargasite and phlogopite) are very common, usually interstitial to other minerals. Plagioclase, interstitial to olivine, is rarely present (Plate VI-d).

4. Mineral chemistry

Compositions of minerals were determined by one of the authors (M. K.), using SEM (Akashi a-30A) with an energy dispersive spectrometer at Kanazawa University.

Olivine has grain-to-grain homogeneity in C-type peridotites, Fo_{91} to Fo_{92} (Fig. 2). In contrast to this, composition of olivine in F-type peridotites is variable from sample to sample, Fo_{89} to Fo_{93} (Fig. 2). This range of Fo content in olivine of our samples examined is equivalent to the value for the least metasomatized peridotites of all Iraya peridotites (Fo_{80-92}) by Schiano et al. (1995). Cr# of chromian spinel is limited in C-type peridotites, 0.5 to 0.6, and is relatively variable in F-type peridotites, 0.4 to 0.7 (Fig. 2). C-type peridotites are within the olivine-spinel mantle array of Arai (1987, 1994) (Fig. 2). The C-type peridotites are similar to mantle residual harzburgite, almost equivalent to the most refractory group of the abyssal peridotites (e. g., Dick and Bullen, 1984 ; Arai, 1994). F-type peridotites are scattered on the Fo-Cr# plane, and part of them are off the olivine-spinel mantle array (Fig. 2).

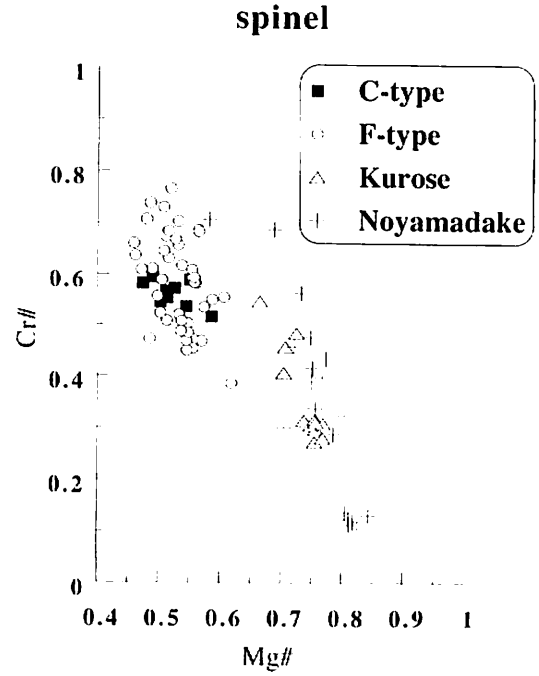

Fig. 4. Relationship between Mg# (= Mg/(Mg + Fe^{2+}) atomic ratio) and Cr# (= Cr/(Cr + Al) atomic ratio) of chromian spinels in the peridotite xenoliths from Iraya volcano, the Philippines. Chromian spinels in peridotite xenoliths from Kurose and Noyamadake, the Southwest Japan arc (Arai and Hirai, 1983 ; Hirai, 1986), are plotted for comparison.

Fe^{3+}/(Cr + Al + Fe^{3+}) atomic ratio of spinel is around 0.1 in F-type peridotites and is a little lower than 0.1 in C-type peridotites (Fig. 3). Relationship between Cr# and Mg# (= Mg/(Mg + Fe^{2+}) atomic ratio) is almost linear and is concordant with the relation in peridotite xenoliths from Kurose (Arai and Hirai, 1983 ; Arai, unpublished) and Noyamadake (Hirai, 1986) from Southwest Japan (Fig. 4). It appears that two (high-Mg# and low-Mg #) trends are distinguished in the Iraya peridotites on the Mg#-Cr# plane (Fig. 4). Almost all C-type peridotites comprise the low-Mg# trend. Apparent Mg-Fe^{2+} partition coeffi-

cients between olivine and chromian spinel are shown in Fig. 5. Two trends are again distinguished; C-type peridotites mostly have higher K_D's than F-type ones (Fig. 5). The high K_D and low K_D trends are almost equivalent to the Kurose and Noyamadake trends, respectively (Fig. 5).

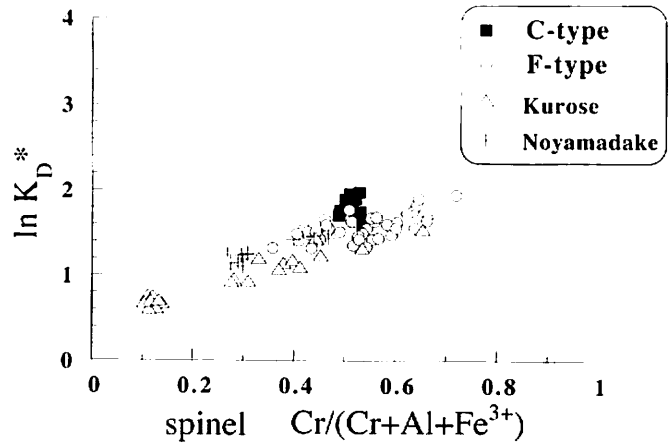

Fig. 5. Apparent Mg-Fe^{2+} partition coefficients between olivine and chromian spinel in terms of Cr/(Cr + Al + Fe^{3+}) atomic ratio of chromian spinel in the peridotite xenoliths from Iraya, Kurose and Noyamadake. Data of Kurose and Noyamadake xenoliths are after Arai and Hirai (1983) and Hirai (1986). $K_D=(Mg/Fe)_{olivine}(Fe/Mg)_{spinel}$. * means a correction for Fe^{3+} after the method of Evans and Frost (1975). Note that C-type peridotites have higher K_D than F-type ones at a given Cr ratio of spinel.

Compositions of orthopyroxene have a contrast between the C-type and F-type peridotites. Orthopyroxene in the C-type peridotite has higher content of CaO (Fig. 6). Al_2O_3 and Cr_2O_3 contents are also higher in C-type peridotites than in F-type ones (Fig. 7). This is basically consistent with the compositional relation in the Tari-Misaka contact aureole ; orthopyroxene in orthopyroxene-olivine zone (the highest-temperature metamorphic zone) is markedly low in CaO, Al_2O_3 and Cr_2O_3 than in harzburgite protolith, which is (the lowest-temperature zone) (Arai, 1974, 1975) (Fig. 7). Mg/(Mg + Fe*) (Fe*, total iron) atomic ratio of orthopyroxene is almost equal to that of coexisting olivine in all samples examined: Mg-Fe partition coefficients between olivine and orthopyroxene are almost unity for both types, indicating an equilibrium for Mg-Fe distribution (Matsui and Nishizawa, 1974).

Plagioclase is highly calcic, up to An_{98} in composition. It coexists with Mg-rich olivine (Fo_{90}).

5. Geothermo-barometry

Two-pyroxene thermometer of Wood and Banno (1973) yields temperatures from 1,050 to 1,200℃ irrespective of peridotite types. Compositional profiles across grain boundaries between a thick lamella and its orthopyroxene host or between discrete two pyroxenes show that they are homogeneous for Ca or Al contents even near the boundaries, indicating the equilibrium. Mg#-Cr# relationship (Fig. 4) and Mg-Fe^{2+} distribution between olivine and spinel (Fig. 5), however, suggest that most of C-type peridotites have lower temperatures

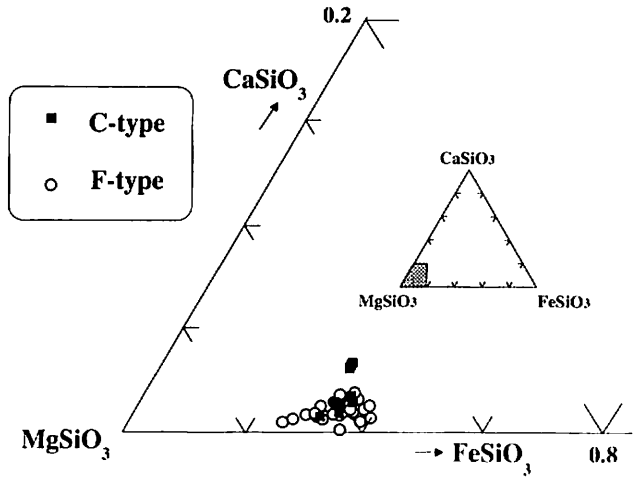

Fig. 6. Ca-Mg-Fe (total iron) atomic ratios of orthopyroxenes in the peridotite xenoliths from Iraya volcano, the Philippines.

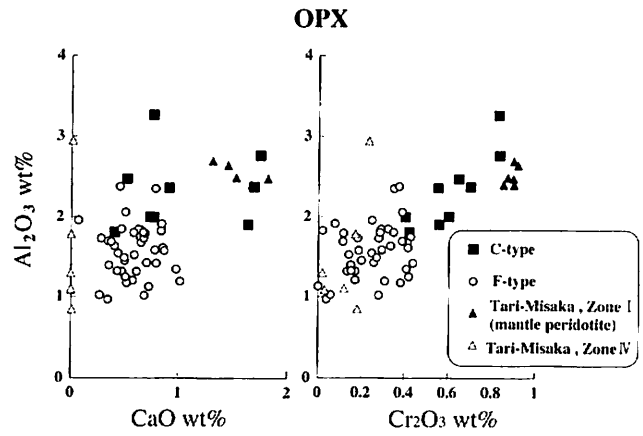

Fig. 7. Compositional relations of orthopyroxenes in the peridotite xenoliths from Iraya volcano, the Philippines, and the deserpentinized peridotites from contact aureole of the Tari-Misaka serpentinite complex (Arai, 1974, 1975). Note that the relation between the C-type and F-type peridotites of Iraya is similar to that between the Zone I (thermally unmetamorphosed ; mantle peridotite) and Zone IV (orthopyroxene-olivine zone) metaperidotites from the Tari-Misaka complex, respectively.

than F-type ones. The coexistence of Ca-rich plagioclase with Mg-rich olivine (PlateVI-d) in some of F-type peridotites means their derivation of shallow upper mantle (<30km) (Kushiro and Yoder, 1966).

6. Discussion

The F-type peridotites are extraordinary as peridotite xenoliths in terms of texture as described before. Their derivation of the upper mantle is guaranteed by the high equilibration temperatures (1,050 to 1,200℃) and spinel peridotitic mineral assemblage with or without Ca-rich plagioclase.

There are two possibilities for their origin, (1) dehydration and (2) Si-metasomatism. The dehydration origin is suggested by their textural and chemical similarities to peridotites formed by dehydration of serpentinite (= deserpentinization), e. g., to metaperidotites of forsterite-enstatite zone from serpentinite masses intruded by granitic magmas (e. g., Arai, 1975). The radial aggregate of orthopyroxene, which is free of deformation and exsolution of diopside, is especially noteworthy (e. g., Plate V-e, f). The dirty appearance of olivine due to minute inclusions is also common to both peridotites (Plate V-d). Relatively low contents of Ca, Al and Cr in orthopyroxene

are also common to them (Fig. 7). The compositional relationship for orthopyroxene between C-type and F-type peridotites from Iraya volcano basically mimics the relation between the metaperidotite of forsterite-enstatite zone and the unmetamorphosed peridotite (mantle peridotite) from thermally metamorphosed serpentinite mass (e. g., Arai, 1975). If the F-type peridotite is deserpentinized peridotite, the C-type peridotite is the protolith of the serpentinite before the dehydration.

The second possibility, the Si-rich melt/fluid metasomatism origin, is suggested by the textures implying replacement in F-type peridotites (e. g., Plate IV-c, d). Orthopyroxene in F-type to intermediate type peridotites often makes flake (Plate IV-d), veinlet (Plate IV-e, f) or network (Plate V-h) cutting or replacing olivine, probably indicating invasion of Si-rich melt/fluid which reacted with olivine to form orthopyroxene. The corroded appearance of coarse olivine in contact with orthopyroxene in F-type peridotites (Plate IV-c) may have also been formed by consumption of olivine due to reaction of Si-rich melt/fluid. The common occurrence of hydrous minerals, phlogopite and hornblende, in F-type peridotites (e. g., Plate V-f ; Plate VI-c) may indicate an involvement of metasomatic agent enriched with incompatible elements in their formation.

We prefer the first possibility, the deserpentinization origin for the F-type peridotite. We think the textures indicative of replacement of olivine by orthopyroxene was possible in deserpentinization process. If deserpentinization occurred at high temperatures, expelled H_2O-rich fluids should have contained large amount of SiO_2 (Nakamura and Kushiro, 1974), which could react with olivine to form secondary orthopyroxene. If F-type peridotites are of metasomatic origin, high-Ca mantle orthopyroxene can coexist with low-Ca metasomatic orthopyroxene, which is not the case in any F-type peridotites. Some of F-type peridotites with gray speckles are very similar in appearance to alpine-type harzburgite partially or totally serpentinized (Plate VI-g, h). The gray speckles in the F-type peridotites are very similar in size and mode of distribution to orthopyroxene or its psuedomorph in alpine-type serpentinites (compare Plate VI-e, f with Plate VI-g, h). The gray speckles, which are composed of secondary low-Ca orthopyroxene with fine-grained inclusions of olivine and chromian spinel, in the F-type peridotites are, therefore, possibly peudomorphs after primary mantle orthopyroxene.

We think that the dehydration of serpentinite or partially serpentinized peridotite is one of important processes in deep parts of young arcs which were developed on oceanic lithosphere. In such a setting the arc magmatism thermally and chemically modifies pre-existing oceanic rocks (e. g., Kay and Kay, 1985). After the pioneering work by Hess (1962) serpentinite or serpentinized peridotite is expected to be an important constituent of the oceanic lithosphere (e. g., Cannat, 1993). Incipient magmatism or diapiric uprise of hot asthenosphere will enhance thermal gradient beneath a young arc on oceanic lithosphere to dehydrate serpentinite. Deserpentinized peridotite xenoliths were also reported from Avacha volcano of Kamchatka arc (Shcheka, 1976). Peridotites of dehydration origin, that is dehydrated oceanic serpentinites, are thus probably present beneath the arcs

developed on oceanic lithosphere such as the Aleutian arc (e. g., Kay and Kay, 1985).

The metasomatic features imposed on Iraya peridotites reported by Maury et al. (1992) and Schiano et al. (1995) are possibly due to high-temperature silicate-bearing fluids expelled either from the magmas as the thermal source of the deserpentinization or from the dehydrated serpentinite.

7. Summary and conclusions

1. Peridotite xenoliths enclosed by calc-alkaline andesite of Iraya volcano, Batan Island, the Philippines, can be classified into two types, C (= coarse-grained)-type and F (= fine-grained type), in terms of texture.

2. C-type peridotites are ordinary harzburgite with equigranular to porphyroclastic textures. Fo content of olivine is 91 to 92 and Cr# of spinel is 0.5 to 0.6. C-type peridotites are similar to the most refractory group of abyssal peridotites. F-type peridotites have extraordinary textures as mantle peridotites and are similar both in texture and mineral chemistry to deserpentinized peridotites from contact aureole. Orthopyroxene in F-type peridotites, which frequently makes radial aggregates, is lower in Ca, Al and Cr contents than that in C-type ones.

3. F-type peridotites are of deserpentinization origin from abyssal serpentinite of which protolith was equivalent to the C-type peridotite. Dehydration of abyssal serpentinite may be one of important processes beneath the young arc which was formed on the oceanic lithosphere.

Acknowledgements

Field assistance by M. V. Manjoorsa and F. Jumawan, University of the Philippines, is greatly acknowledged. I. Matsumoto helped us to prepare figures. R. C. Maury gave S. A. information of Batan island and xenoliths.

References

Abe, N. and Arai, S. (1993). Petrographical characteristics of ultramafic xenoliths from Megata volcano, the Northeast Japan arc. *Sci. Rept. Kanazawa Univ.*, v. 38, p. 1-24.

_____, _____ and Saeki, Y. (1992). Hydration processes in the arc mantle; petrology of the Megata peridotite xenoliths, the Northeast Japan arc. *Jour. Mineral. Petrol. Econ. Geol.*, v.87, p. 305-317 (in Japanese with English abstract).

_____, _____ and Ninomiya, A. (1995a). Peridotite xenoliths and essential ejecta from the Ninomegata crater, the Northeastern Japan arc. *Jour. Mineral. Petrol. Econ. Geol.*, v. 90, p. 41-49 (in Japanese with English abstract).

_____, _____ and Yurimoto, H. (1995b). Petrology of the uppermost mantle beneath the island arc and its

relationship with arc magmatism. *Proceed. Todai Symp. 1995 "The role of magmas in the evolution of the Earth", Tokyo*, p. 98-99.

Aoki, K. and Prinz, M. (1974). Chromian spinels in lherzolite inclusions from Itinome-gata, Japan. *Contrib. Mineral. Petrol.*, v. 18, p. 326-337.

Arai, S. (1974). "Non-calciferous" orthopyroxene and its bearing on the petrogenesis of ultramafic rocks in Sangun and Joetsu zones. *Jour. Japan. Assoc. Min. Pet. Econ. Geol.*, v. 69, p. 343-353.

_____ (1975). Contact metamorphosed dunite-harzburgite complex in the Chugoku district, western Japan. *Contrib. Mineral. Petrol.*, v. 52, p. 1-16.

_____ (1987). An estimation of the least depleted spinel peridotite on the basis of olivine-spinel mantle array. *N. Jb. Miner. Mh.*, p. 347-354.

_____ (1991). Petrological characteristics of the upper mantle peridotites beneath the Japan Island arcs − Petrogenesis of spinel peridotites−. *Soviet Geol. Geophys.*, v. 32, p. 8-26.

_____ (1994). Characterization of spinel peridotites by olivine-spinel compositional relationships : Review and interpretation. *Chem. Geol.*, v. 111, p. 191-204.

_____ and Hirai, H. (1983). Petrographical notes on deep-seated and related rocks (1) Mantle peridotites from Kurose and Noyamadake alkali basalts, southwestern Japan. *Ann. Rep. Inst. Geosci. Univ. Tsukuba*, v. 9, p. 65-67.

Cannat, M. (1993). Emplacement of mantle rocks in the seafloor at mid-ocean ridges. *Jour. Geophys. Res.*, v. 98, p. 4163-4172.

Dick, H. J. B. and Bullen, T. (1984). Chromian spinel as a petrogenetic indicator in abyssal and alpine-type peridotites and spatially associated lavas.*Contrib. Mineral. Petrol.*, v. 86, p. 54-76.

Evans, B. W. and Frost, B. R. (1975). Chrome-spinel in progressive metamorphism - a preliminary analysis. *Geochim. Cosmochim. Acta*, v. 39, p. 952-972.

Hayashi, H. (1955). Ejecta around Ichinome-gata in Oga Peninsula, Akita Prefecture. *Jour. Geol. Soc. Japan*, v. 61, p. 240-248 (in Japanese).

Hess, H. H. (1962). History of ocean basins. In: Engel, A. E. J., James, H. L. and Leonard, B. F. (Ed.) Petrologic Studies, Burlington Volume,, p. 599-620, Geol. Soc. America, Boulder, Colo.

Hirai, H. (1986). *Petrology of ultramafic xenoliths from Noyamadake and Kurose, southwestern Japan.* Unpublished D. Sc. thesis, University of Tsukuba. p. 181.

Irving, A. J. (1980). Petrology and geochemistry of composite ultramafic xenoliths in alkalic basalts and implications for magmatic processes within the mantle. *Amer. Jour. Sci.*, v. 280-A, p. 389-426.

Kay, S. M. and Kay, R. W. (1985). Role of crystal cumulates and the oceanic crust in the formation of the lower crust of the Aleutian arc. *Geology*, v. 13, p. 461-464.

Kuno, H. and Aoki, K. (1970). Chemistry of ultramafic nodules and their bearing on the origin of basaltic magmas. *Phys. Earth Planet. Interiors*, v. 3, p. 273-301.

Kushiro, I. and Yoder, H. S., Jr. (1966). Anorthite-forsterite and anorthite-enstatite reactions and their bearing on the basalt-eclogite transformation. *Jour. Petrol.*, v. 7, p. 337-362.

Matsui, Y. and Nishizawa, O. (1974). Iron (II)-magnesium exchange equilibrium between olivine and calcium-free pyroxene over a temperature range 800℃ to 1300℃. *Bull. Soc. fr. Minéal. Cristallogr.* v. 97. p. 112-130.

Matsumoto, I., Arai, S., Muraoka, H. and Yamauchi, H. (1995). Petrological characteristics of the dunite-harzburgite-chromitite complexes of the Sangun zone, Southwest Japan. v. 90. p. 13-26. *Jour. Mineral. Petrol. Econ. Geol.*, (in Japanese with English abstract).

Maury, R. C., Defant, M. J. and Joron, J.-L. (1992). Metasomatism of the sub-arc mantle inferred from trace

elements in Philippine xenoliths. *Nature*, v. 360, p. 661-663.

Nakamura, Y. and Kushiro, I. (1974). Composition of the gas phase in Mg_2SiO_4-SiO_2-H_2O at 15 kbar. *Carnegie Inst. Washington Year Book*, v. 73, p. 255-258.

Ninomiya, A. and Arai, S. (1992). Harzburgite fragment in a composite xenolith from an Oshima-Oshima andesite, the Northeast Japan arc. Bull. *Volcanol. Soc. Japan*, v. 37, p. 269-273 (in Japanese).

Nixon, P. H. (1987). Mantle Xenoliths. Wiley Interscience Pub. John Wiley & Sons. Chichester. p. 844.

Richard, M. (1986). *Gêlogie et Pêtrologie d'un Jalon de L'arc Taïwan-Luzon : L'île de Batan (Philippine).* Thèse de doctrat, Univ. Bretagne Occidentale (in French with English abstract).

_____, Maury, R. C., Bellon, H., Stephan, J. F., Boirat, J. -M. and Calderon, A. (1986). Geology of Mt. Iraya volcano and Batan island, northern Philippines. *Phil. Jour. Volcanol.*, v. 3, p. 1-27.

Schiano, P., Clocchiatti, R., Shimizu, N., Maury, R. C., Jochum, K. P. and Hofmann, A. W. (1995). Hydrous, silica-rich melts in the sub-arc mantle and their relationship with erupted arc lavas. *Nature*, v. 377. p. 595-600.

Shcheka, S. A (1976). Evidence of metamorphism of ultramafic inclusions before incorporation into basalt magma. *Dokl. Akad. Nauk USSR*, v. 227, p. 704-707.

Stephan, J. F., Blanchet, R., Rangin, C., Pelletier, B., Letouzey, J. and Muller, C. (1986). Geodynamic evolution of the Taiwan-Luzon-Mindoro belt since the late Eocene. *Tectonophys*. v. 125, p. 245-268.

Takahashi, E. (1978). Petrologic model of the crust and upper mantle of the Japanese island arcs. *Bull. Volcanol.*, v. 41, p. 529-547.

_____ (1980). Thermal history of lherzolite xenoliths - Petrology of lherzolite xenoliths from the Ichinomegata crater, Oga Peninsula, northeast Japan, Part I. *Geochim. Cosmochim. Acta*, v. 44, p. 1543-1658.

_____ (1986). Genesis of calc-alkali andesite magma in anhydrous mantle-crust boundary : petrology of lherzolite xenoliths from the Ichinomegata crater, Oga Peninsula, northeast Japan, part II. *Jour. Volcanol. Geotherm. Res.*, v. 29, p.355-395.

Vidal, P., Dupuy, C., Maury, R.C. and Richard, M. (1989). Mantle metasomatism above subduction zones : trace-element and radiogenic isotope characteristics of peridotite xenoliths from Batan Island (Philippines). *Geology*, v. 17, p. 1115-1118.

Wood, B. J. and Banno, S. (1973). Garnet-orthopyroxene and orthopyroxene-clinopyroxene relationships in simple and complex systems. *Contrib. Mineral. Petrol.*, v. 42, p. 109-124.

Captions for Plates

Xenoliths from Iraya volcano of Batan island, the Philippines. Scale bars in photomicrographs are 0.5mm.

Plate I

fig. a Iraya volcano from a southern slope near Basco, Batan island.
fig. b An outcrop of pyroclastic flow deposits at Song-Song Bay.
fig. c The pyroclastic flowdeposit enriched with blocks and xenoliths at Song-Song Bay. P, peridotite. G, gabbro.
fig. d A block of andesite (No. NC1) with a peridotite xenolith, which is rimmed by dark hornblendite. Note small dark aggregates of hornblende in andesite, which are possibly digested peridotite.
fig. e A block of andesite (E4) with an accidental andesite xenolith (left) and a C-type peridotite xenolith, which composite with dark gabbro at the left side.
fig. f Photomicrograph of an olivine-free andesite block (No. S13) which contains peridotite xenoliths. Note the prominent zonal structure of plagioclase phenocryst. Plane-polarized light.
fig. g Photomicrograph of an olivine-bearing andesite block (No. S19) which hosts peridotite xenoliths. Plane-polarized light.
fig. h Photomicrograph of an andesite host (No. S78), which includes hornblende without opacite rim. Plane-polarized light.

Plate II

fig. a The largest peridotite xenolith (F-type ; No. E8), weighing 5.6 kg.
fig. b Gabbro-peridotite composite xenoliths from Iraya volcano (left ; No. E2) and from Oshima-Oshima volcano (right). Note the similar appearance of the two xenoliths.
fig. c A gabbro xenolith with peridotite clasts with hornblendite selvages (No. S20). Note the color difference of peridotite between the left clasts (paler) and the right ones (darker).
fig. d A gabbro xenolith with hornblendite clasts, which are possible completely reacted peridotite. No. S29.
fig. e A composite xenolith (No. S56). F-type peridotite cut by honblendite network, which is as a whole enclosed by gabbro.
fig. f A peridotite xenolith (No. S37-1) with gabbro-hornblendite selvage in andesite host.
fig. g A radial aggregate of orthopyroxene (arrow) in a peridotite of F-type (No. S62-8).
fig. h Photomicrograph of aggregates of orthopyroxene with numerous inclusions of olivine and other minerals in a peridotite of F-type (No. S-17). Crossed-polarized light.

Plate III

fig. a A peridotite xenolith (C-type ; No. E13) with hornblendite selvage. Note the coarse-grained texture of the peridotite.
fig. b A peridotite xenolith (F-type ; No. S6) with gray speckles. Black dot is chromian spinel a light green is clinopyroxene. Note the difference in appearance between C-type peridotite (a) and F-type peridotite (b).
fig. c Photomicrograph of a typical C-type peridotite (S71-1) with porphyroclastic texture. Note that orthopyroxene porphyroclast which is kinked and has exsolution lamellae of clinopyroxene. Crossed-polarized light.
fig. d Photomicrograph of a typical F-type peridotite (S29-3) with fine-grained olivine. Crossed-polarized light. Note the difference with C-type peridotite (c).
fig. e The color difference between F-type peridotite clast (F ; paler) and C-type one (C ; darker). A gabbro-peridotite composite xenolith (No. S20).
fig. f Well-developed clinopyroxene exsolution lamellae in orthopyroxene porphyroclast in a peridotite of C-type (No. E34-1). Crossed-polarized light.
fig. g Clinopyroxene (cpx) associated with chromian spinel in a peridotite of C-type (No. S71-1). Plane-polarized light.
fig. h Anhedral chromian spinel associated with orthopyroxene in a peridotite of F-type (No. S71-1). Plane-polarized light.

Plate IV

fig. a Fine-grained olivine aggregate surrounded by hornblendite at the lower marginal part of fig. h of Plate V (peridotite cut by network of orthopyroxenite and hornblendite) (No. S29-3). Plane-polarized light.

fig. b Fine-grained olivine aggregate surrounded by orthopyroxenite in peridotite-orthopyroxenite-hornblendite composite xenolith (No. S29-3 ; fig. h of Plate V).

fig. c Photomicrograph of an intermediate type of peridotite (No. S66), which has fine-grained olivine aggregate (left), coarse olivine (right to upper center) and radial aggregate of orthopyroxene (center). Note the coarse olivine embayed by orthopyroxene. Plane-polarized light.

fig. d Orthopyroxene crystals replacing olivine in a peridotite of F-type (No. E19-12). Note the relic olivine in orthopyroxene (center). Crossed-polarized light.

fig. e Thin orthopyroxene veinlet cutting olivine-rich part of a peridotite of F-type (No. S64-9). Crossed-polarized light.

fig. f Orthopyroxenite vein in olivine-rich part in a peridotite of F-type (No. S22). Note the boundaries of the vein is complicated. Crossed polarized light.

fig. g Orthopyroxenite vein in olivine-rich part in a peridotite of F-type (No. S62-3). Crossed-polarized light.

fig. h Plane-polarized light. Note that the spinel was split and patrly included by the vein.

Plate V

fig. a Possible fluid inclusion trails in olivine in a peridotite of C-type (No. E34-1). Plane-polarized light.

fig. b Crossed-polarized light. Minute orthopyroxene dots (arrows) are arranged with possible fluid inclusions.

fig. c An intermediate type of peridotite (E1-5) which has coarse olivine grains in fined-grained matrix of olivine.

fig. d Fine olivine in a peridotite of F-type (S29-3) with frequent minute inclusions. Note that the marginal part of each olivine grain is free from inclusions. Plane-polarized light.

fig. e Photomicrograph of a radial aggregate of orthopyroxene, which is free of clinopyroxene lamellae and is full of minute inclusions, in a peridotite of F-type (No. S64-5). Note the interstitial phlogopite. Crossed-polarized light.

fig. f Plane-polarized light.

fig. g Photomicrograph of a radial aggregate of orthopyroxene, which is free of clinopyroxene lamellae and is full of olivine and magnetite inclusions, in a meta-peridotite from orthopyroxene-olivine zone in Kasamatsu serpentinite complex intruded by granitic magma, Southwest Japan (see Matsumoto et al., 1995). Crossed-polarized light. Note the similarity with the orthopyroxene aggregate of F-type peridotites from Iraya (fig. e).

fig. h A peridotite xenolith of F-type with a network of orthopyroxenite (brown) and hornblendite (dark green) (No. S29-3).

Plate VI

fig. a Photomicrograph of the a gray speckle in a peridotite of F-type (No. S64-5). It consists of orthopyroxene with minute inclusions and subordinate amount of olivine. Plane-polarized light.

fig. b Crossed-polarized light.

fig. c Chromian spinel which was fragmented and has interstitial phlogopite in a peridotite of F-type (No. S76-3). Plane-polarized light.

fig. d Plagioclase interstitial to olivine in a peridotite of F-type (intermediate type) (No. S63-5). Crossed-polarized light.

fig. e A peridotite xenolith of F-type with gray to green speckles (No. S60-1). The speckles are mainly composed of orthopyroxene.

fig. f A peridotite xenolith of F-type with gray speckles and black dots (chromian spinel) (No. S1-1).

fig. g A weathered block of partly serpentinized harzburgite from the northern Kamuikotan belt, Hokkaido, Japan. Greenish speckles are orthopyroxene porphyroclasts which have survived from serpentinization. Note that the appearance is very similar to F-type peridotite xenoliths from Iraya volcano (figs. e and f above).

fig. h A weathered block of serpentinized harzburgite from the northern Kamuikotan belt, Hokkaido,

Japan. Dark green speckles are pseudomorphs of orthopyroxene. Note that the appearance is very similar to F-type peridotite xenoliths from Iraya volcano (figs. e and f above).

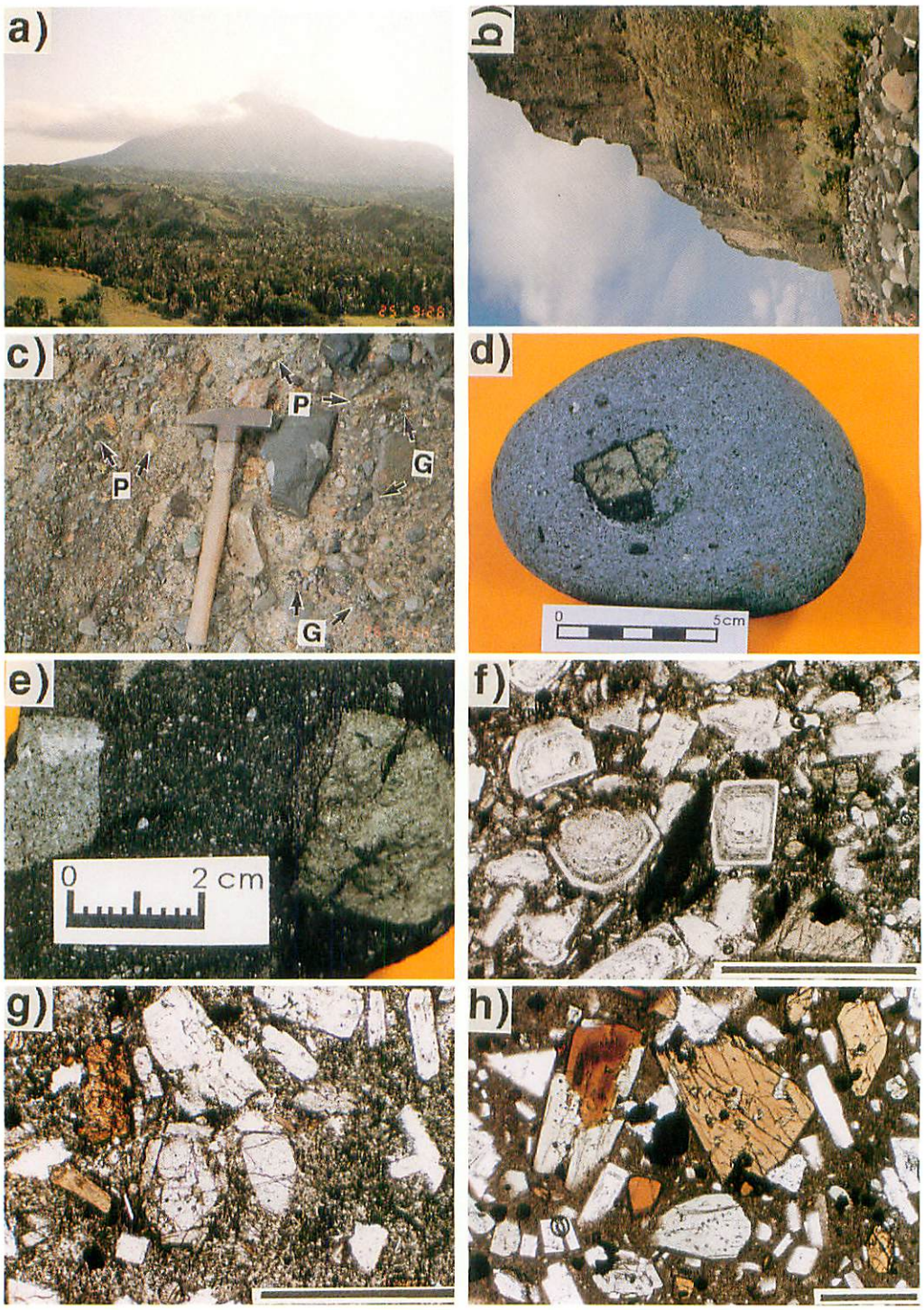
a)
b)
c)
P
P
G
G
d)
0
5cm
e)
0
2 cm
f)
g)
h)

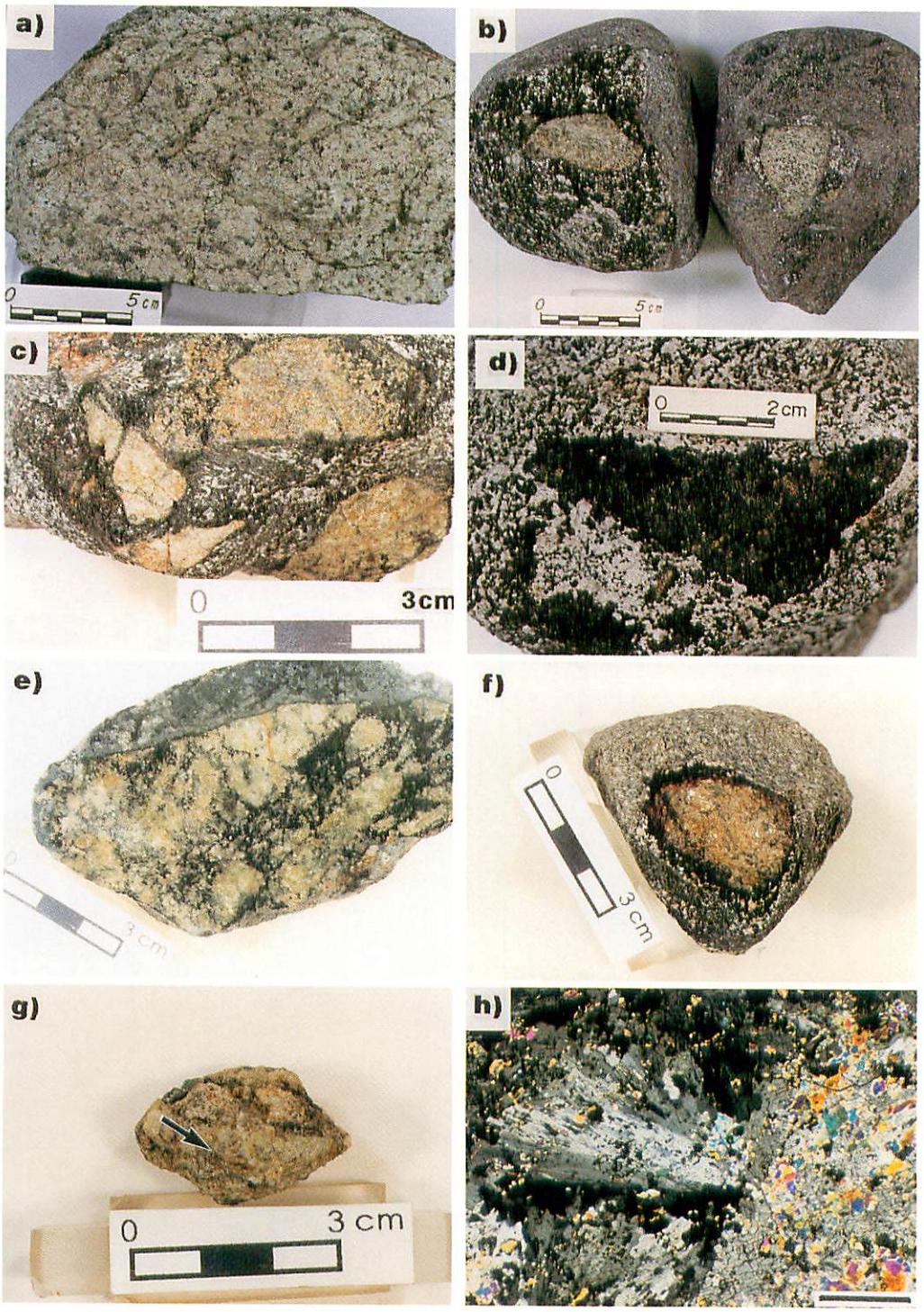
a)
0 5cm
b)
0 5cm
c)
0 3cm
d)
0 2cm
e)
0 3cm
f)
0 3cm
g)
0 3 cm
h)

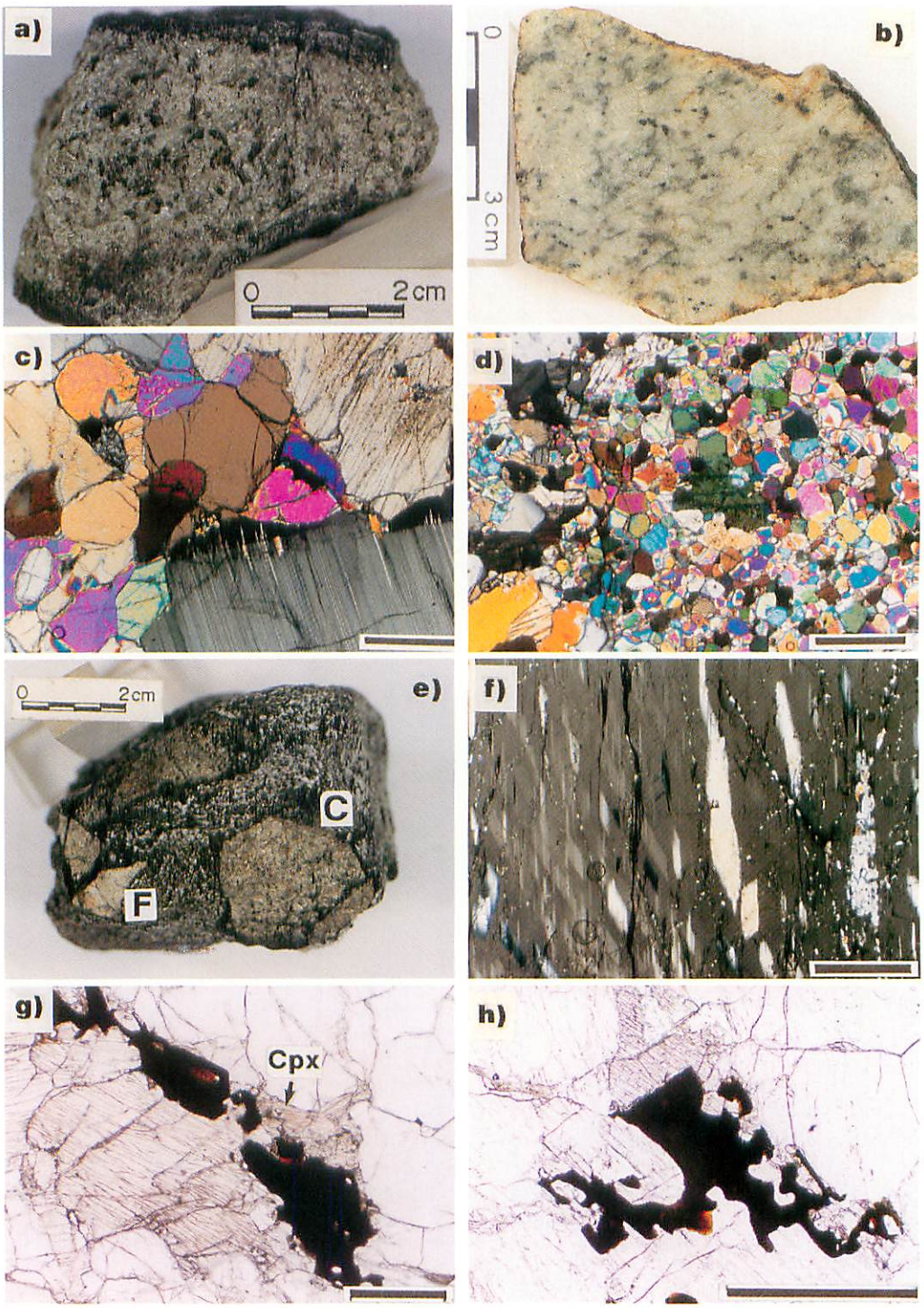
a)
0 2cm
b)
0 3cm
c)
d)
e)
0 2cm
C
F
f)
g)
Cpx
h)

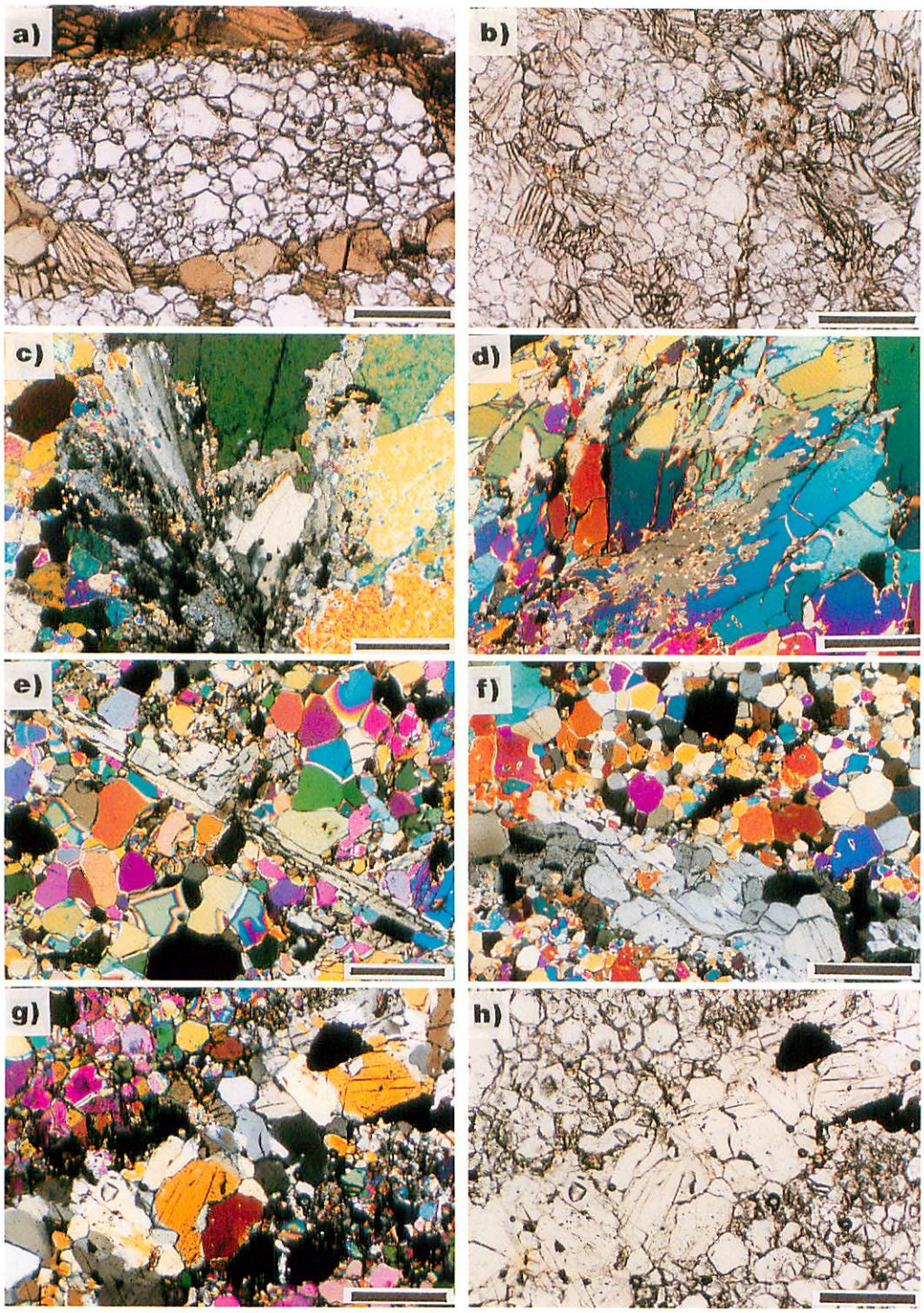
a)
b)
c)
d)
e)
f)
g)
h)

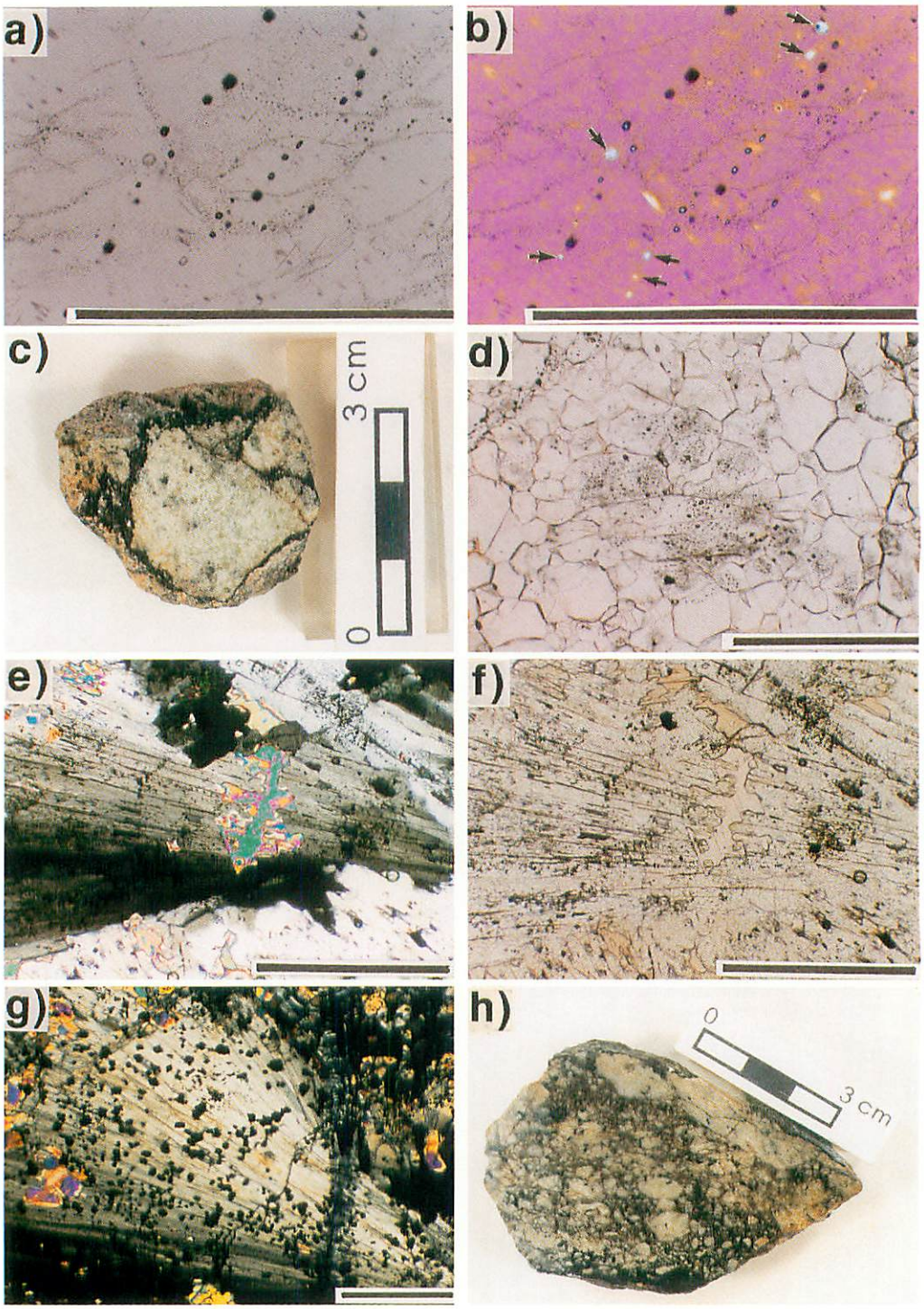
a)
b)
c)
3 cm
0
d)
e)
f)
g)
h)
0
3 cm

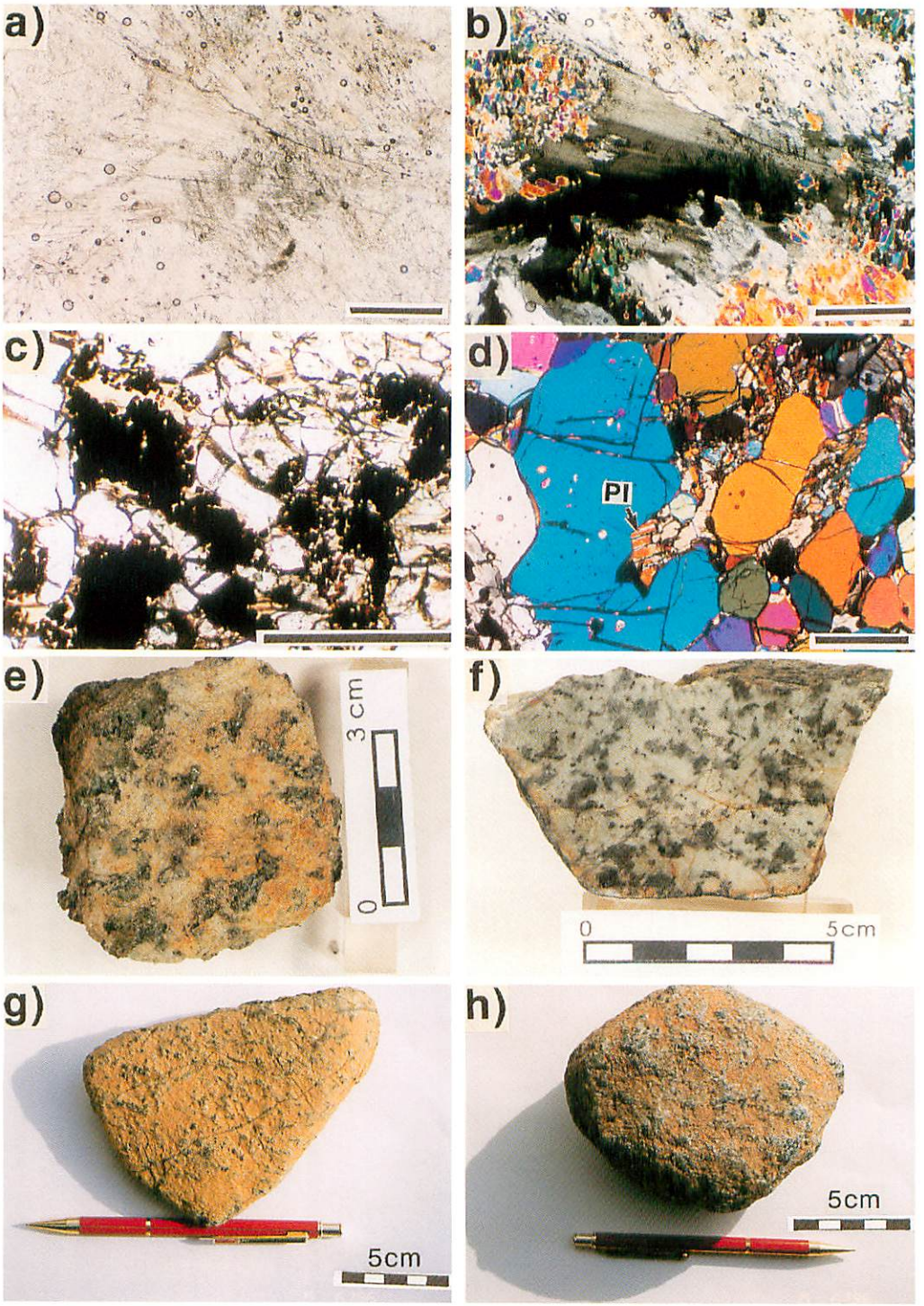
a)
b)
c)
d)
Pl
e)
3 cm
0
f)
0
5cm
g)
5cm
h)
5cm